Journal of Engineering Physics and Thermophysics, Vol. 74, No. 5, 2001

NUMERICAL MODELING OF THE THERMAL AND GASDYNAMIC STRUCTURE OF PLASMA FLOWS IN ELECTRIC-ARC REACTORS WITH THREE-JET MIXING CHAMBERS

L. I. Krasovskaya and M. A. Brich

UDC 533.915:001.573

On the basis of a three-dimensional mixing model of plasma jets, a numerical study is made of the gasdynamic and thermal structure of plasma flows in three-jet mixing chambers of several types and in cylindrical reactors with such chambers. It is shown that in cylindrical chambers (with a diameter of 5–10 cm) and in a conic chamber with an apex angle of 60° (with a base diameter of 10 cm) for diameters of plasmatron nozzles of 1–2 cm the mixing of plasma jets proceeds virtually completely in the chamber volume. Application of such chambers provides the formation of rather uniform (in cross sections) temperature fields in the channels of plasma reactors.

Electric-arc plasma reactors find wide application in various technological processes. The application of multijet electric-arc reactors is characterized by the combination of the possibility of building up rather simply the power of a heating unit with the possibility of controlling the gasdynamic and thermal structure of the flows formed and the conditions of mixing of the flows with raw material. The basic unit of such reactors is a cylindrical or conic mixing chamber on which a few (most often three) plasmatrons symmetrically installed on the side surface of the chamber operate. A mixing chamber is arranged, as a rule, in the upper part of a reactor; the chamber is followed by a water-cooled channel of the reactor. In connection with the objective difficulties encountered in an experimental study of high-temperature flows, which are complicated in structure and composition and are confined by the walls of the plasma reactor, it is expedient to combine experiment with numerical modeling. In so doing, for multijet reactors it is necessary to develop mathematical models which describe the spatial inhomogeneity of the parameters of a plasma flow in the reactor. The replacement of local injections over the channel perimeter by a continuous circular source performed, for instance, in [1] simplifies a numerical study of the fluid dynamics of a multijet reactor; however it disregards the complexity of the object studied. The actual gas flow in such reactors is three-dimensional and turbulent.

In modeling axisymmetric turbulent plasma flows, the k–ε turbulence model [2–14], the model of a mixing path [12, 15, 16], and the "two-fluid" model [17], which allows the discontinuity and the non-mixing phenomena in a turbulent plasma flow, have been adopted. Of these turbulence models, the k–ε model should be recognized as the most universal one; therefore, we have used precisely this model in developing a three-dimensional model of plasma flows in reactors with three-jet mixing chambers.

The differential equations for the heat transfer and fluid dynamics of plasma flows can be represented in a generalized vector form as

$$\partial (\rho\Phi)/\partial t + \operatorname{div} (\rho \mathbf{v}\Phi) = \operatorname{div} (\Gamma_\Phi \operatorname{grad} \Phi) + S_\Phi \,. \tag{1}$$

The diffusion coefficients Γ_Φ and the source terms S_Φ of the basic equations of the three-dimensional model of plasma flows are given in Table 1.

Academic Scientific Complex "A. V. Luikov Heat and Mass Transfer Institute," National Academy of Sciences of Belarus, Minsk, Belarus. Translated from Inzhenerno-Fizicheskii Zhurnal, Vol. 74, No. 5, pp. 108–114, September–October, 2001. Original article submitted February 13, 2001.

1062-0125/01/7405-1201$25.00

TABLE 1. Diffusion Coefficients Γ_Φ and Source Terms S_Φ of the Equations of a Three-Dimensional Model of Turbulent Plasma Jets and Flows

Equations of	Variable Φ	Diffusion coefficient Γ_Φ	Source terms S_Φ
Continuity	1	0	0
Motion	$\mathbf{v}$	0	$-\text{grad}\, p + \mathbf{F} + \rho\mathbf{g} + \rho\mathbf{a}$
Energy	$v^2/2 + e$	η/σ_h	$-\text{div}\,(p\mathbf{v}) + \rho(\mathbf{gv})$
Turbulence energy	k	η/σ_k	$G - \rho\varepsilon$
Dissipation of the turbulence energy	ε	η/σ_ε	$(\varepsilon/k)(C_1 G - C_2\rho\varepsilon)$

The generalized variable Φ denotes the velocity components, the total energy of a gas, equal to the sum of the internal and kinetic energies ($e + v/2$), the kinetic energy of turbulence k, and the dissipation rate of the turbulence energy ε. The effective viscosity coefficient η is equal to the sum of the coefficients of molecular (η_m) and turbulent (η_t) viscosity. In the k–ε model of turbulence, $\eta_t = C_D\rho k^2/\varepsilon$. For empirical constants, the values $C_1 = 1.43$, $C_2 = 1.92$, $C_D = 0.09$, $\sigma_k = 1$, $\sigma_h = 0.9$, and $\sigma_\varepsilon = 1.3$, which have been recommended by Spalding and Pan and tested in two-dimensional modeling of plasma flows [2, 6, 8, 9, 11, 13, 18, 19], are adopted.

The channels of flow plasma reactors are usually of a cylindrical shape; therefore, the mathematical formulation of the problem and its solution were carried out using a cylindrical coordinate system (r, φ, t). An expression establishing the relationship between the generation rate of turbulence energy G and the spatial gas-velocity distribution was obtained based on the hypothesis of a cascade mechanism, in conformity with which the kinetic energy of a turbulent flow dissipates according to the following scheme: the kinetic energy of macroscopic motion of a flow $\rightarrow$ the energy of turbulent pulsations $\rightarrow$ the energy of thermal motion of molecules. The quantity G can be determined as the divergence-free (dissipation) side of the expression for the work of viscosity forces per unit time $A = v_1F_1 + v_2F_2 + v_3F_3$. After carrying out substitution of the components F_1, F_2, and F_3 of the vector of the force of viscous resistance expressed in terms of the tensor of viscous stresses, a number of transformations, and separation of the divergence of convolution of the vector $\mathbf{v}$ and the tensor of viscous stresses τ, we obtain

$$A = \text{div}\,(\mathbf{v}\tau) + \eta\,[2\,(\partial_1 v_1)^2 + 2\,(\partial_2' v_2)^2 + 2\,(\partial_3 v_3)^2 + (\partial_1 v_2 + \partial_2' v_1)^2 + (\partial_1 v_3 + \partial_3 v_1)^2 +$$

$$+ (\partial_2' v_3 + \partial_3 v_2)^2 + 3v_1/r\,\partial_2' v_2 - 2v_2/r\,(\partial_1 v_2 - \partial_2' v_1) + 2\,(v_1/r)^2 + (v_2/r)^2] = \text{div}\,(\mathbf{v}\tau) + G\,, \qquad (2)$$

where $\partial_1 \equiv \partial/\partial r$, $\partial_2 \equiv \partial/\partial\varphi$, $\partial_3 \equiv \partial/\partial z$, and $\partial_2' \equiv \partial_2/r$.

The equations of dynamics are solved simultaneously with the equations of state of a gas. For the density of the internal energy and the mean molar mass of air, we used the dependences $e = e(\rho, T)$ and $M = M(T)$ corresponding to the local thermodynamic equilibrium. As the boundary conditions, we used the values of the temperatures and the mass flow rates of a plasma arriving from the plasmatron nozzles and of the pressure at the reactor inlet and outlet. On the walls, the adherence conditions and the local densities of a heat flux were prescribed. In calculating heat transfer, we assumed that the density of the heat flux toward the walls is $q_w = \alpha(T_w - T_0)$. The heat-transfer coefficient α was determined from the value of the integral heat loss to the reactor walls per unit time:

$$\alpha = \frac{(1 - \eta_r)\,W}{\int (T_w - T_0)\,dS}\,. \qquad (3)$$

In constructing a discrete (in space) analog of the considered system of differential equations, the flow region was overlapped by a calculational grid formed by three families of the surfaces: r = const, φ = const, and z = const. The unit cell of the calculational grid represented a cylindrical sector. In the calculations of the reactors with conic chambers, the conic surfaces were approximated by a set of cylindrical surfaces, which coincide in height with the height of the calculational cells in each horizontal layer, and by radii equal to the radius of the conic surface at a height corresponding to the center of the layer. The scalar parameters of state of a gas (density ρ, pressure p, temperature T, internal-energy density ρe, density of the kinetic energy of turbulence ρk, density of the dissipation rate of the kinetic energy of turbulence $\rho\varepsilon$) were assumed to be prescribed at the centers of the cells, while the components of the velocity vector were prescribed at the centers of the faces perpendicular to the corresponding component. Discretization over space implies the approximation of the initial system of partial equations (1) for the generalized vector variable Φ considered as a function of time t and three spatial coordinates r, φ, z by a system of ordinary differential equations describing the time dependence of the parameters of state at the indicated points. The convective terms of the equations were approximated by the "counterflow" difference scheme. Integration of the equations with respect to time was carried out by the Runge–Kutta method. The time step of integration Δt was calculated in the course of counting. The difference scheme used belongs to a class of explicit difference schemes; therefore, Δt has been chosen so as to ensure the stability of the computational process, which is determined by the Courant–Hilbert conditions: $\Delta t < \Delta x/(v_s + |v|)_{\max}$. The quantity $(v_s + |v|)_{\max}$ represents a maximum value for the sum of the local velocity of sound and of the absolute value of the flow velocity.

The method of solution used was checked by calculating test one- and two-dimensional problems of motion of a liquid and a gas similar to those represented in [20] and having analytical solutions, and also by carrying out two-dimensional calculations of the temperature fields in plasma jets [21], for which experimental and calculated data have been published [14].

To evaluate the influence of the geometric parameters of mixing chambers on the structure of plasma flows formed, a series of simultaneous calculations for several versions of mixing chambers and reactors with a length of 50 cm (including the mixing chamber) was performed. The width of the reactors coincided with the base diameter of the chambers. The height of cylindrical chambers was 11 cm; the height of conic chambers was determined by the angle of opening of the cone. The centers of the inlet holes for plasmatrons were arranged symmetrically on the level of the mid-height of the mixing chambers. Plasma jets were injected perpendicularly to the side surface of the chambers. With the gas flow rates being the same in the plasmatrons (without a swirl), the problem is symmetric. In this case, the two most differing longitudinal sections of the temperature and velocity fields are the sections passing through the plasmatron axis and between two plasmatrons at equal distances from the latter. The corresponding azimuthal angles of the section planes (reckoning is from the axis of one plasmatron) are $\varphi = 0^o$ and $\varphi = 30^o$. The plasma temperature at the reactor inlet is assumed to be equal to 5000 K; the pressure at the reactor inlet and outlet is 10^5 Pa; the air flow rate via each of the plasmatrons is 3 g/sec; heat loss in the cylindrical mixing chambers amounts to 20%, in the conic chambers to 15%, and in the reactor channels to 15% of the power supplied to the reactor.

The developed package of programs allows visualization of a probable picture of a gas flow in plasma apparatuses and determination of its temperature fields. In describing calculation results, we will use the abbreviated notation of mixing chambers following the pattern C-50-10-90, where C indicates cylindrical (Co is conic); 50 is the diameter of the chamber base, mm; 10 is the diameter of plasmatron nozzles, mm; 90 is the angle of injection of jets with respect to the chamber axis directed downward, deg. The isotherms on the graphs are numbered in accordance with the temperature growth in the direction from the walls to the high-temperature zones. Certain isotherms are not denoted because of insufficient spatial resolution.

Calculations for the C-50-10-90, C-50-20-90, C-100-10-90, and C-100-20-90 chambers have demonstrated that the cylindrical mixing chambers are characterized (especially for 10-mm diameters of plasmatron nozzles) by a rather uniform radial temperature profile at the outlet, with the exception of small near-wall

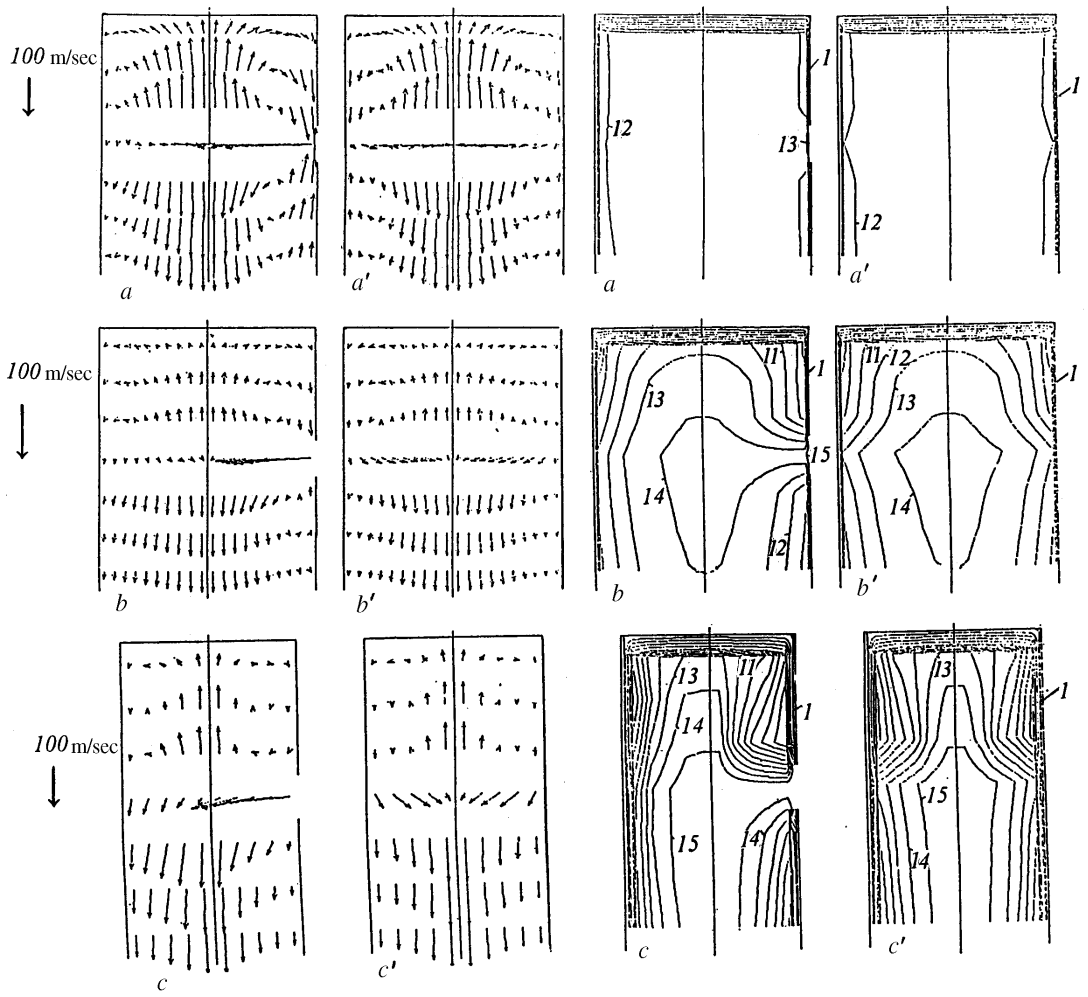

Fig. 1. Velocity and temperature fields in C-100-10-90 (a, b), C-100-20-90 (b, b′), and C-50-10-90 (c, c′) mixing chambers; the gas flow rate through each plasmatron is 3 g/sec; the initial plasma temperature is 5000 K; the isotherms drawn are: 1) 500; 2) 1000; 3) 1500; 4) 2000; 5) 2500; 6) 3000; 7) 3200; 8) 3400; 9) 3600; 10) 3800; 11) 4000; 12) 4200; 13) 4400; 14) 4600; 15) 4800 K; the azimuthal angles of the longitudinal sectional planes (reckoning is from the axis of one plasmatron) are $\varphi = 0^o$ (a, b, c) and $\varphi = 30^o$ (a′, b′, c′).

portions, over which the temperature abruptly decreases (Fig. 1). The longitudinal velocities have maxima on the chamber axis, which is associated with both the higher gas flow rate in the central part of the chamber and its higher temperature. In the cylindrical chambers, the inflow of the external gas is absent, according to the calculations, which provides maintenance of the high temperature of the flow at the outlet. In the C-50-10-90 chamber, the volume is almost totally filled with a gas with a temperature of 4200–4600 K, while in the C-100-10-90 chamber, the volume is filled with a gas with a temperature of 4200 K.

Three-jet mixing chambers are applied in certain cases for forming a plasma flow flowing out into open space with its further use for some other purposes (for instance, for investigation of the behavior of bodies in high-temperature flows). In plasma-chemical reactors, the plasma flow usually arrives at the reactor channel. The calculations have shown that the temperature and velocity fields in cylindrical reactors in the zones corresponding to mixing chambers are almost identical to those calculated for the corresponding cham-

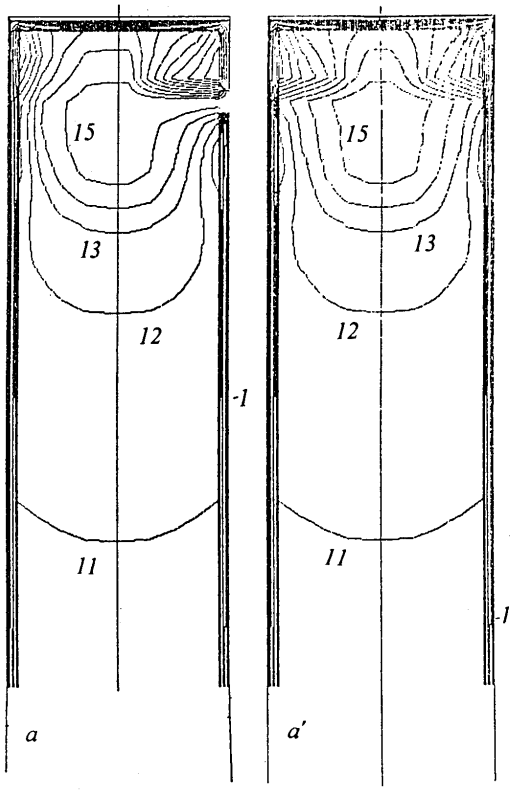

Fig. 2. Temperature fields in the reactor with a C-50-20-90 mixing chamber; the gas flow rate via each plasmatron is 3 g/sec; the initial plasma temperature is 5000 K; in constructing the projections, use is made of the scaling factor decreasing the reactor length in relation to its width by a factor of three; the drawn isotherms are identical to those in Fig. 1; the azimuthal angles of the longitudinal sectional phases (reckoning is from the axis of one of the plasmatrons) are $\varphi = 0^o$ (a) and $\varphi = 30^o$ (a′).

bers, from which the plasma flow flows out into open space. Over a length of 1–2 calibers from the plane of injection of the jets, plasma flows with a uniform radial temperature distribution and with a rather uniform velocity distribution in the central part of the reactor are formed (Fig. 2). As a consequence of the heat transfer with the walls, the enthalpy of the gas flow along the reactor channel abruptly decreases, which is manifested as changes in the temperature fields.

Calculations for an initial plasma temperature of 5000 K and an air flow rate of 3 g/sec via each of the plasmatrons have shown that the situation in the conic mixing chambers with a perpendicular attachment of the plasmatrons to the chamber surface is determined to a considerable degree by the angle of opening of the cone, correspondingly, by the angle of injection of the jets with respect to the chamber axis (Figs. 3 and 4). In the Co-100-20-30 chamber, the gas velocities in the radial direction in the plane passing through the centers of the holes intended for injection of plasma jets have low values. The basic volume of the chamber is occupied by a gas with a temperature < 2500 K since the plasma jets move only over limited peripheral portions. As the jets do not undergo mixing, the gas temperatures and velocities at the chamber outlet have complicated radial profiles. In the sections passing through the plasmatron axes ($\varphi = 0^o$), the profiles have maxima displaced toward the chamber wall. With increase in the angle of injection of the plasma jets up to 45^o with respect to the chamber axis (Co-100-20-45) and up to 60^o (Co-100-20-60), the gas velocities in the radial direction in the plane passing through the centers of the holes intended for injection of plasma jets

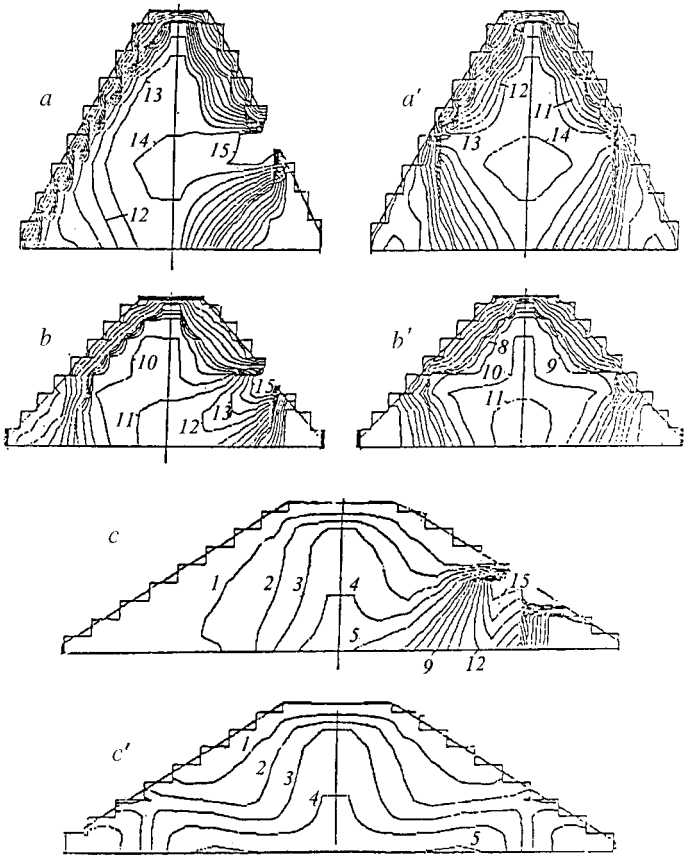

Fig. 3. Isotherms of the gas in Co-100-20-60 (a), Co-100-20-45 (b), and Co-100-20-30 (c) conic mixing chambers; the gas flow rate via each plasmatron is 3 g/sec; the initial plasma temperature is 5000 K; the drawn isotherms are similar to those in Fig. 1; the azimuthal angles of the longitudinal sectional planes (reckoning is from the axis of one plasmatron) are $\varphi = 0^o$ (a, b, c) and $\varphi = 30^o$ (a′, b′, and c′).

increase. Here, the volume occupied by a high-temperature gas in the chamber increases; the radial profiles of the temperatures at the outlet of the chambers have a maximum at the center of the section.

The high level of the gas temperature at the outlet of the mixing chambers makes it possible to employ spectral methods for its measurement, in particular, the method based on determination of the relative intensity of spectral components [22]. For an air plasma generated by plasmatrons with copper electrodes, the line pairs CuI 510.5/521.8 nm and 510.5/515.3 nm are convenient. They lie in close proximity in the spectrum, thus allowing one not to carry out heterochromic photometric measurements. An energy difference of 2.35 eV of the upper levels of the chosen lines is sufficiently great; therefore, it leads to an insignificant error in temperature measurements. Spectral studies of the temperature of plasma flows at a distance of 1 mm from the outlet sections of three-jet mixing chambers are described in [23, 24]. For the 11-cm-high C-50-20-90 chamber (with the radial injection of jets via symmetrically arranged holes on the level of the mid-height), a uniform temperature profile of the air-plasma flow is obtained almost over the entire channel section (Fig. 5). For the conic three-jet mixing chambers with plasmatrons perpendicularly attached thereto, it has been established that in injection of jets at an angle of 60^o to the chamber axis, the high-temperature part of the flow leaving the Co-100-20-60 chamber is concentrated near the reactor axis; the radiation intensity over the periphery is small. With decrease in the angle of injection of the jets with respect to the chamber axis up to 45 and 30^o, the asymmetry of the radiation intensity over the section has been observed.

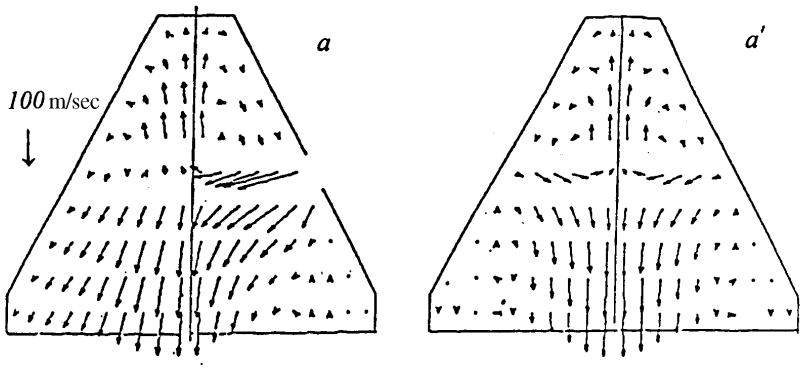

Fig. 4. Velocity fields of the gas in a Co-100-20-60 mixing chamber; the gas flow rate via each plasmatron is 3 g/sec; the initial temperature of a plasma is 5000 K; the azimuthal angles of longitudinal sectional planes (reckoning is from the axis of one plasmatron) are $\varphi = 0^o$ (a) and $\varphi = 30^o$ (a′).

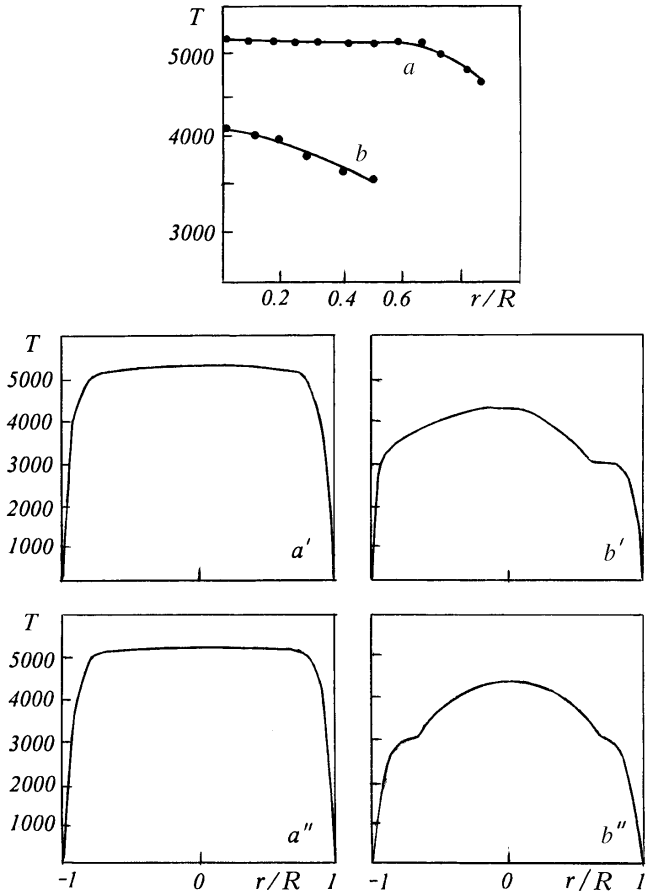

Fig. 5. Spectral (a, b) and calculated (a′, a″, b′, b″) radial temperature profiles of the plasma flow on the lower cuts of cylindrical C-50-20-90 (a) and conic Co-100-20-60 (b) mixing chambers; the initial mass-mean temperature of the plasma is 5450; the gas flow rate via each of the plasmatrons is 2 (a) and 3 (b) g/sec; the azimuthal angles of longitudinal sectional planes (reckoning is from the axis of one plasmatron) are $\varphi = 0^o$ (a′, b′) and $\varphi = 30^o$ (a″, b″).

Numerical calculations have been performed for several regimes similar to those used in the spectral investigations. For the cylindrical C-50-20-90 chamber, in calculations as well as in the experiment, a two-dimensional temperature profile has been obtained for the central high-temperature part of the flow, which occupies the area at the reactor outlet corresponding to more than 60% of the chamber diameter (Fig. 5). In the cylindrical chambers, the inflow of the external gas is absent, as the calculations show, which provides maintenance the high temperature of the flow at the outlet of the C-50-20-90 chamber. According to the calculations, a distinctive feature of the considered conic chambers not connected to the reactor channel is the inflow of the external gas and the formation of return flows at the outlet of the chambers (Fig. 4). This fact is consistent with the considerable temperature decrease recorded by spectral measurements at the outlet of the Co-100-20-60 chamber as compared to the initial mass-mean plasma temperature (Fig. 5). If the return flows ($v_z < 0$) develop in the outlet section, then for the corresponding cells at the chamber outlet it is necessary to prescribe the values of the scalar parameters ρ, ρe, ρk, and $\rho\varepsilon$ as the boundary conditions. The results shown in Fig. 5 are obtained with the use, as such parameters, of the mass-mean values of ρ, ρe, ρk, and $\rho\varepsilon$ averaged over those cells of the outlet section for which $v_z > 0$.

In the conic chambers, the zones of return flows are formed at the bottom underneath the plasmatrons; therefore, on their articulation with the reactor channel, the temperature fields undergo more pronounced changes than in the reactors with cylindrical chambers. Below the indicated zones the plasma flows are characterized by rather uniform radial distributions of temperatures and velocities for the major part of the cross sections of the reactors.

Thus, the structures of three-jet reactors with channel diameters of 5–10 cm and anode nozzles of the plasmatrons of 1–2 cm provide a high efficiency of mixing of the plasma jets in the case of their radial injection, which favors the equalization of the heat-transfer conditions for the basic mass of raw material and the attainment of a high yield of the target products. Among the conic chambers discussed, the Co-100-20-60 chamber provides higher temperatures in the zone of collision of the jets, which makes it preferable for technological purposes.

NOTATION

t, time; ρ, density; $\mathbf{v}$, velocity vector; v_1, v_2, and v_3, radial, azimuthal, and axial components of the velocity vector; Φ, generalized variable; e, internal energy of the gas; k, kinetic energy of turbulence; ε, dissipation rate of the turbulence energy; p, gas pressure; $\mathbf{F}$, force of viscous resistance; $\rho\mathbf{g}$, external mass force; $\rho\mathbf{a}$, force of inertia; G, generation rate of the turbulence energy; η, effective coefficient of viscosity; q_w, density of the heat flux toward the walls; α, heat-transfer coefficient; η_r, thermal efficiency of the reactor; W, useful power supplied to the reactor with a plasma; T_w, gas temperature in the near-wall region; T_0, temperature of the water cooling the reactor; S, area of the reactor walls; Δx, space step of the calculational grid; v_s, local velocity of sound.

REFERENCES

1. V. V. Berbasov, V. P. Lukashov, B. A. Pozdnyakov, et al., in: *Plasmachemical Processes* [in Russian], Moscow (1979), pp. 138–154.
2. A. Dilawari and J. Szekely, *Plasma Processing Synthesis Mater.*, **98**, 3–19 (1987).
3. Y. C. Wei, B. Farouk, and D. A. C. Apelian, *Plasma Processing Synthesis Mater.*, **98**, 41–47 (1987).
4. D. J. Varacalle, L. D. Reynolds, and C. B. Shaw, *Plasma Processing Synthesis Mater.*, **98**, 49–60 (1987).
5. Y. Lee and E. Pfender, *Plasma Chem. Plasma Processing*, **7**, No. 1, 1–27 (1987).
6. A. Dilawari and J. Szekely, *Plasma Chem. Plasma Processing*, **7**, No. 3, 317–339 (1987).

7. Y. P. Chyou and E. Pfender, *Plasma Chem. Plasma Processing*, **9**, No. 2, 291–328 (1989).
8. M. M. Jankovic, D. Z. Milojevic, and P. Lj. Stefanovic, *Colloque de Physique*, **51**, C5-229–C5-236 (1990).
9. C. H. Chang and E. Pfender, *Plasma Chem. Plasma Processing*, **10**, No. 3, 493–500 (1990).
10. C. H. Chang and J. D. Ramshaw, *Plasma Chem. Plasma Processing*, **13**, No. 2, 189–209 (1993).
11. P. B. Pavlovic, G. S. Zivkovic, P. Lj. Stefanovic, and A. V. Saljnikov, in: *Proc. 2nd Eur. Congr. on Thermal Plasma Processes*, Vol. 1, Paris (1992), pp. 381–388.
12. D. Lengerken, Z. Janasz, and D. Hebecker, *VDI Berichte 1166*, 575–582 (1995).
13. G. Simard, M. Bouios, and A. Charette, *VDI Berichte 1166*, 97–104 (1995).
14. J. McKelliget, J. Szekely, M. Vardelle, and P. Fauchais, *Plasma Chem. Plasma Processing*, **2**, No. 3, 317–326 (1982).
15. P. Proulx, J. Mostaghimi, and M. I. Boulos, in: *Proc. 8th Int. Symp. on Plasma Chemistry*, Tokyo (1987), pp. 13–18.
16. P. Proulx, J. Mostaghimi, and M. I. Boulos, *Colloque de Physique*, **51**, C5-263–C5-270 (1990).
17. P. C. Huang, J. Heberlein, and E. Pfender, *Plasma Chem. Plasma Processing*, **15**, No. 1, 25–46 (1995).
18. O. P. Solonenko and A. L. Sorokin, *VDI Berichte 1166*, 129–136 (1995).
19. M. Sijercic, V. Vujovic, and A. Saljnikov, *VDI Berichte 1166*, 565–572 (1995).
20. P. M. Kolesnikov and M. A. Brich, in: *Mathematical Models of the Theory of Transfer in Inhomogeneous and Nonlinear Media with Phase Transformations* [in Russian], Minsk (1986), pp. 3–25.
21. L. I. Krasovskaya and M. A. Brich, in: *Proc. IV Minsk Int. Forum "Heat and Mass Transfer — MIF-2000,"* 22–26 May, 2000 [in Russian], Vol. 4, Minsk (2000), pp. 138–145.
22. H. B. Griem, *Plasma Spectroscopy* [Russian translation], Moscow (1969).
23. A. L. Mossé and I. S. Burov, *Processing of Dispersed Materials in Plasma Reactors* [in Russian], Minsk (1980).
24. A. L. Mossé, *Electric-Arc Plasma Reactors with Three-Jet Mixing Chambers* [in Russian], Preprint No. 19 of the Heat and Mass Transfer Institute of the BSSR Academy of Sciences, Minsk (1990).